Modification and Stabilization of Collapsible Loess using Diammonium Phosphate Solution

Chengjuan Ying , Lingxia Huang * , Haiming Chen * , Yadong Zhang , Duoxi Yao

Posted Date: 12 April 2024

doi: 10.20944/preprints202404.0835.v1

Keywords: loess; hydroxyapatite; soil stabilization; compressive strength; diammonium phosphate

 doi:10.20944/preprints202404.0835.v1

Article

Modification and Stabilization of Collapsible Loess Using Diammonium Phosphate Solution

Chengjuan Ying [1], Lingxia Huang [2,*], Haiming Chen [3,*], Yadong zhang [3] and Duoxi Yao [1]

[1] School of Earth and Environment, Anhui University of Science and Technology, Huainan, China; xiaoying790514@163.com (C.Y.); dxyao@aust.edu.cn (D.Y.)
[2] College of Civil Engineering, Fuzhou University, Fuzhou, China
[3] Engineering Research Center of Underground Mine Construction, Ministry of Education (Anhui University of Science and Technology), Huainan, China; 15256020693@163.com
* Correspondence: 1095674659@qq.com (L.H.); 2009028@aust.edu.cn (H.C.)

Abstract: The collapsible loess will rapidly soften and lose its bearing capacity when soaked in water. Under a mild condition (20°C), the biomimetic inorganic agent, Diammonium phosphate (DAP), reacts with calcite in the collapsible loess, producing a stronger bonding material, hydroxyapatite (HAP), to modify and stabilize the soil. Uniaxial compression, permeability tests and morphological analysis using XRD and SEM/EDX microscopy were carried out to assess the effectiveness of DAP stabilization on the collapsible loess. The results indicated that HAP improved the inter-particle bonding within loess, filled the pores within particles, reduced the permeability, and consequently mitigated collapsibility of loess. The compressive strength of DAP-treated loess increased as DAP concentration increased. Following 28-days curing, the compressive strength of the loess treated with a 3.0 mol/L DAP solution was six times greater than that of the untreated group. DAP's reinforcement effect on loess was superior to that of cement. The compressive strength of DAP-treated loess was about double that of cement-treated loess and the permeability coefficient was reduced by more than 50% at equivalent solid content. Furthermore, DAP generated 68% fewer carbon emissions compared to Portland cement. Considering eco-friendly and sustainable development, DAP offers a more competitive alternative for modification and stabilization of loess.

Keywords: loess; hydroxyapatite; soil stabilization; compressive strength; diammonium phosphate

1. Introduction

Loess, widely distributed in the Loess Plateau in Western China [1,2], forms as loose sediment under the arid and semi-arid climatic conditions of the Quaternary period [3–5]. The soil particles in loess primarily consist of fine silt fine silt, and the interparticle spaces within skeleton particles are rich in soluble carbonate components. These components bond the particles together, forming various aggregates of loess. As a result, loess is loose and porous with strong permeability. Despite demonstrating high strength in arid conditions, loess exhibits extremely poor water stability and unique collapsibility [6–8]. When exposed to water, the bonding materials between skeleton of loess particles dissolve and fail, leading to internal structural disintegration. Consequently, the strength rapidly diminishes, and uneven additional subsidence occurs due to external loads or self-weight. This phenomenon can result in unstable building foundations and structural damage in engineering projects. Although loess is widely used as filling material of foundation [9], its susceptibility to collapse poses significant challenges for construction.

Dynamic compaction and cement/lime modification are two traditional soil improvement methods of collapsible loess foundations. Dynamic compaction uses the dynamic effect of heavy hammer's impacts to enhance the loess's stability. The process encourages a denser rearrangement of the loess particles' skeleton, with gradual infilling of the pores. However, dynamic compaction

 doi:10.20944/preprints202404.0835.v1

cannot address the solubility of the bonding materials between loess particles. Even after compaction, the loess can still exhibit collapsibility once it is exposed to water for a period.

Cement or lime can effectively modify the structural properties of loess and enhance its mechanical properties [10]. This soil stabilization method involves mixing lime or cement into the soil to increase its strength. Cement stabilize the collapsible loess through various chemical reactions, including ion exchange, cement hydration and hardening, flocculation and aggregation, etc. Horpibulsuk et al. [11] studied the changes in the micro-structure of cement-modified silty clay after 7-day curing. Their findings indicated that the bonding between soil particle aggregates was enhanced and the soil's pores were diminished because of cement hydration, which consequently improved the soil's strength and structural properties. Lemaire et al. [12] observed the micro-structure of lime and cement-modified plastic silty soil for 28-day curing time. Following the addition of cement, the soil particles were completely covered and stronger cemented by a layer of bonding material, resulting in a significant enhancement of the modified soil's strength and water stability[13].

Although cement modification can effectively mitigate the collapsibility of loess [14], the production of cement is energy-intensive and results in the substantial emission of carbon dioxide into the atmosphere. Cement, as a primary source of carbon emissions, is responsible for about 9% of the total industrial carbon emissions in China. Chinese government has actively pledged to peak carbon dioxide emissions by 2030 and to realize carbon neutrality by 2060 [15]. To achieve these objectives, it is essential to explore innovative eco-friendly stabilization methods or materials for collapsible loess that could serve as a sustainable alternative to cement [16–18]. These methods also enable conserving resources, safeguarding the environment, diminishing expenditures, and shortening the construction timeline [19,20].

The loess's engineering properties are significantly affected by the type and interparticle bonds between the skeleton of loess particles and aggregates [21–23]. In loess, the carbonate cementing material mainly exists in the form of calcite, significantly contributing to the soil's strength [24–26]. Furthermore, the calcium carbonate is a highly effective binder that can react with phosphates [27]: phosphate ions can interact with calcium ions released from calcite in aqueous solutions, resulting in the precipitation of hydroxyapatite (HAP) crystals.

HAP, which possesses the chemical formula $Ca_{10}(PO4)_6(OH)_2$, serves as an inorganic repair and modification material with broad application prospects [28]. Its nanoscale crystal structure closely resembles that of calcite, with better chemical stability, lower solubility, higher strength and stiffness. In some ancient monuments and churches, it has been discovered that some oxalate and apatite coatings were added artificially to protect the course substrate from environmental erosion [24,29].Yang Fuwei et al. [30] and Sena da Fonseca et al. [31] have treated marble by brushing, dripping, or immersing it in diammonium phosphate (DAP, the chemical formula $(NH_4)_2HPO_4$) solutions to prepare the precipitation of HAP. The generated protective HAP coatings have a good adhesion strength and effectively improve the acid and alkali corrosion resistance of marble. E. Sassoni et al. [32] have experimentally demonstrated that phosphates can also effectively stabilize soil materials.

A commonly used consolidation or stabilization method involves reacting DAP with either the soil itself or externally added carbonates to generate HAP for modifying and stabilizing the soil. Under mild temperature conditions (10-20°C), DAP solution can react with calcium ions to form HAP complexes [25], which improve the interparticle bonding strength in soil. This effectively increases the strength of binder between loess particles and fills the surrounding pores. The chemical reaction is as follows [25]:

$$10CaCO_3+5(NH_4)_2HPO_4 \rightarrow Ca_{10}(PO_4,CO_3)_6(OH,CO_3)_2+5(NH_4)_2CO_3+3CO_2+2H_2O \quad (1)$$

The formation process of HAP complexes is mild and non-exothermic, allowing it to fill pores without causing additional soil deformation. Loess, being a natural weakly alkaline saturated soil rich in calcium carbonate, can sufficiently react with DAP and generate HAP complexes without the necessity of adding an external calcium source. However, during the precipitation reaction, if a large amount of phosphates binds to the surfaces of carbonate-containing soil particles through adsorption

 doi:10.20944/preprints202404.0835.v1

and ion exchange, it may reduce the activity of surface calcium ions. This, in turn, may promote the formation of various amorphous calcium phosphate (CP) phases rather than HAP, diminishing the reinforcing effect on the soil. In the precipitation reactions of HAP complexes, it is generally believed that the calcium-to-phosphorus (Ca/P) molar ratio of approximately 1.18 is conducive to the formation of amorphous calcium phosphate [33,34]. Increasing the Ca/P molar ratio during the reaction can favor the formation of HAP, and at Ca/P molar ratio of 1.5, calcite crystals can be completely transformed into HAP [35].

In this study, we aimed to assess the impact of DAP stabilization on the collapsible loess. To achieve this, the remolded samples were mixed with DAP solutions of varying concentrations, specifically 0.5, 1.0, 1.5, 2.0, and 3.0 mol/L. Additionally, cement-treated loess samples with different cement contents were also prepared under the same curing conditions for comparison. The stabilized performance of the treated loess samples was compared through uniaxial compression tests and permeability tests. Finally, by utilizing micro- analytical techniques such as XRD and SEM/EDX, the structural characteristics of the modified loess were examined to verify the effect and mechanism behind the reaction between DAP solution and calcium carbonate in loess to generate HAP for reinforcing the loess. The research findings offer a novel and competitive option for stabilizing collapsible loess grounds, characterized by efficiency, energy savings, and environmental friendliness.

2. Materials and Methods

2.1. Materials

In this study, analytical-grade diammonium phosphate (DAP) was used. It appears as colorless, transparent monoclinic crystals. It has a solubility of 58 g at 10 °C, and the resulting aqueous solution is alkaline with a pH of 8.0. The cement used in the experiment is P O 42.5, whose density was 1910 kg/m^3 and specific surface area was 1.447 m^2/g. It exhibits low shrinkage during the hardening process, effectively mitigating the occurrence of shrinkage cracks and ensuring reliable test outcomes.

The loess utilized in the experiments was sourced from the Lanzhou, Gansu in Western China, and was classified as silty clay. It falls under the category of fine-grained clay, characterized by its loose appearance without stratification and well-developed pores within its matrix. The soil's bulk unit weight is 1.43, with a specific gravity of 2.71. It has a plastic limit (w_P) of 15.1%, a liquid limit (w_l) of 25.2%, and a plasticity index (I_P) of 10.1. The distribution of grain sizes for this loess is detailed in Table 1. The loess's natural porosity ranges from 52% to 55%, indicating a high potential for collapsibility.

Table 1. The distribution of the loess's grain size.

Grain-Size Fraction	Silty-Fine Sand	Coarse Silt	Fine Silt	Clay
Grain diameter (μm)	>50	10-50	5-10	<5
Content (%)	12.4	61.9	17.3	7.9

The primary chemical composition of the loess, as illustrated in Table 2, includes calcium carbonate/magnesium carbonate and clay minerals, primarily illite and montmorillonite, along with minor amounts of kaolinite. The original soil sample underwent crushing and sieving through a 0.65 mm square-hole sieve to eliminate impurities such as stones and roots. It was then mixed with the stabilization agents and remolded by compaction to prepare the loess samples for the further experimental research.

Table 2. The loess's chemical composition.

Composition	CaO	MgO	Al_2O_3	SiO_2	CO_2	Fe_2O_3
Content (%)	13.0	2.93	12.9	48.0	10.3	6.23

 doi:10.20944/preprints202404.0835.v1

2.2. Methods

To assess the stabilization effects of various agents on loess, experiments were designed in accordance with the "Standard for Geotechnical Testing Method (GB/T 50123-2019)" [36]. The experimental design included the following groups:

- Blank control group (UT) served as the reference without any form of stabilization;
- Cement-treated groups (CM-4, CM-6, CM-8) employed various cement contents to modify and stabilize the loess;
- DAP-treated groups (DT-0.5, DT-1.0, DT-1.5, DT-2.0, DT-3.0) employed different concentrations of DAP solution.

Table 3 provides the specific mix proportions of stabilization agents for each experimental group. DAP treated the loess with its aqueous solution. With a DAP concentration of 3.0 mol/L, the solid content of DAP within the treated loess samples approximated 6.3% by weight. During the reaction between DAP and the soil's calcium carbonate, a Ca/P molar ratio of 4.8 was maintained, theoretically allowing complete conversion to HAP. Considering the time required for the release of calcium ions from calcite, curing is essential to enhance the reaction and improve stabilization effectiveness of the loess samples. The study involved evaluating unconfined uniaxial compressive strength, measuring changes in permeability, and analyzing carbon emissions and costs of stabilization agents. These tests and analyses were conducted to assess the stabilization effects of DAP and cement, as well as their environmental and economic benefits.

Table 3. The mix proportions of stabilization agents.

Groups	Cement Content (wt%)	Molar Concentration of DAP (mol/L)	Water Content (wt%)
UT	0	-	16
CM-4	4	-	
CM-6	6	-	
CM-8	8	-	
DT-0.5	-	0.5	
DT-1.0	-	1.0	
DT-1.5	-	1.5	
DT-2.0	-	2.0	
DT-3.0	-	3.0	

2.2.1. Unconfined Uniaxial Compressive Test

Cylindrical specimens were utilized to conduct the uniaxial compressive strength test on the loess samples. By compacting the remolded loess in a steel mold and then demolding, loess specimens required for unconfined compressive tests were prepared. The unconfined compressive strength test was performed under strain control employing an electro-hydraulic servo uniaxial compression machine, maintaining a loading rate of 1% per minute. The numerical value of the ultimate compressive strength was obtained for each specimen, and the average result for a group of specimens was recorded as the uniaxial compressive strength of that group. The specific procedures for the preparing and curing loess specimens for compressive testing are as follows:

1. The sieved loess was subsequently dried in an oven over 24 hours at a temperature of 105 °C for. After allowing the loess to cool to room temperature, an appropriate amount of cement and water, or an equal volume of DAP solution, were added into the loess according to the optimal moisture content ratio and the mix proportions in Table 3. The mixture was thoroughly blended with water for at least 5-10 minutes to ensure a uniform blend.
2. The mixed loess was then placed into a steel mold with dimensions of 50 mm by 100mm. The loess within the mold was compacted using an electric compactor, and the specimens were removed after their top and bottom surfaces were leveled. The number of compactions for the

 doi:10.20944/preprints202404.0835.v1

remaining groups of loess specimens was based on this standard to maintain the degree of compaction and ensure uniformity in the preparation of the specimens. After compaction, the dry density of the untreated loess specimens should achieve 1.72 g/cm³.

3. To simulate the curing environment of a roadbed, the demolded cylindrical loess specimens were kept inside a curing chamber set to 23 degrees Celsius and 96% humidity. Five specimens were cured as a group for curing periods of 3 d, 7 d, 14 d, and 28 d. After curing, they were transferred to an oven and heated at 105 degrees Celsius until the weight remained constant before removal.

Based on the compaction test results of the loess obtained using an electric compactor, the best moisture level for the remolded loess was measured to be 16±0.5%, with the maximum dry density of the untreated loess specimens reaching 1.72 g/cm³. The void ratio, measured by saturation and drying methods, was found to be within the range of 0.54-0.55.

2.2.2. Permeability Test

To investigate the permeability coefficient changes of modified and remolded loess, variable head permeability tests were conducted. Based on the optimal moisture content, loess flow specimens were prepared:

1. Both untreated loess (control group) and loess treated with cement/DAP were compressed using an electric compactor to achieve maximum dry density. Subsequently, ring samples were extracted from the compressed specimens. These ring samples were subsequently stored in a conditioning room for a specified age.
2. The ring samples were inserted into the container of saturation permeameter, sealed, and connected to a water head. The water was drained until no bubbles were observed in the overflow water. The permeability coefficient test was conducted when the sample saturation exceeded 0.95.
3. At ambient room temperature, the time interval was recorded for the water level's descent from 90 cm to 70 cm. After each measurement, the water head was raised back to the specified height for another measurement. This process was repeated no less than five times. When the inflow and outflow rates stabilized and showed consistency, the calculated permeability coefficient was determined to represent the saturated permeability coefficient.

The formula for calculating the loess's saturated permeability coefficient k_T is:

$$k_T = 2.3\frac{aL}{A(t_1 - t_2)}\lg\frac{H_1}{H_2} \quad (2)$$

In the formula, k_T represents the saturated permeability coefficient (cm/s); a denotes the cross-sectional area of the tube (cm²); A symbolizes the cross-sectional area of the permeameter (cm²); L is the distance traveled by the water, equivalent to the specimen's height (cm); t_1 and t_2 are respectively the initial and final times of the water head readings (s); H_1 and H_2 are the water heads at the start and end times, respectively (m).

After completing the permeability test, the ring samples were removed from the container, and wiped clean of any surface moisture before being weighed. They were subsequently transferred to an oven at 105°C for over 24 hours to achieve complete dryness. Once the mass no longer changed, the samples were taken out and reweighed. The mass loss of the samples was recorded to calculate the volume loss of water after drying the saturated samples, which in turn allowed for the determination of the porosity ratio of the ring samples.

2.2.3. Characterization Analysis

After the completion of the above experiments, soil samples were obtained for subsequent characterization analysis. The loess's primary chemical composition was determined through X-ray fluorescence spectroscopy (XRF). Its crystalline phases were analyzed using a TTR-III θ/θ type high-power XRD instrument with Cu-Kα radiation at 40 kV and 200 mA. The analysis employed a scanning rate 8°/min, covering an angular range from 2θ = 20° to 60°. Samples for analysis were

 doi:10.20944/preprints202404.0835.v1

collected from different internal regions of the loess specimens. Additionally, a JSM-IT100 SEM, functioning at 15 kV with a resolution of 10-20 μm was employed to observe the microsurface morphology of various soil samples.

Additionally, an X-ray scanning (EDX) probe was utilized to analyze the elemental distribution within the samples. Prior to the analysis, the samples were finely milled into powder and uniformly spread on SEM stubs coated with a conductive adhesive. The EDX detector was then used to assess the distribution of various elements on the surface of soil particles. This allowed for an in-depth investigation into how DAP treatment affects the microscopic morphology of the loess particles.

3. Results and Discussion

3.1. Compressive Strength

Figure 1 illustrates the remolded loess specimens treated with different concentrations of DAP. Following the drying process, the density of the DAP-treated loess increased by 1-4%, with the increment dependent on the concentration of DAP. The white crystalline material, such as HAP and other apatite components, observed in the loess specimens, was generated by the ion exchange and adsorption precipitation reactions between DAP and calcium carbonate found both on the surface and embedded within the loess matrix. Consequently, the DAP-treated loess specimens exhibited a whitish appearance. The formation of HAP can enhance the bonding between particles and aggregates within the loess. The efficacy of DAP treatment increased with increasing concentrations of the agent. This resulted in a whiter coloration of the specimen and a notable enhancement in surface hardness.

Figure 2 illustrates the compressive strength of cement-treated loess. The untreated group (UT) exhibited minimal change in compressive strength over the course of curing. However, the compressive strength of cement-treated group (CM) increased with prolonged curing periods. This improvement is attributed to the hydration reactions of the cement, which progressively develop a bonding matrix between soil particles. Cement-modified loess requires an extended curing time (28 d) to maximize its stabilization potential.

As the curing age advanced, the hydration reaction became more complete, resulting in increased cohesion and friction between loess particles. Moreover, the process yielded an increased amount of hydration products, which filled the pore and decreased the soil's porosity. Owing to these effects, the cement-treated loess displayed a substantial improvement in compressive strength.

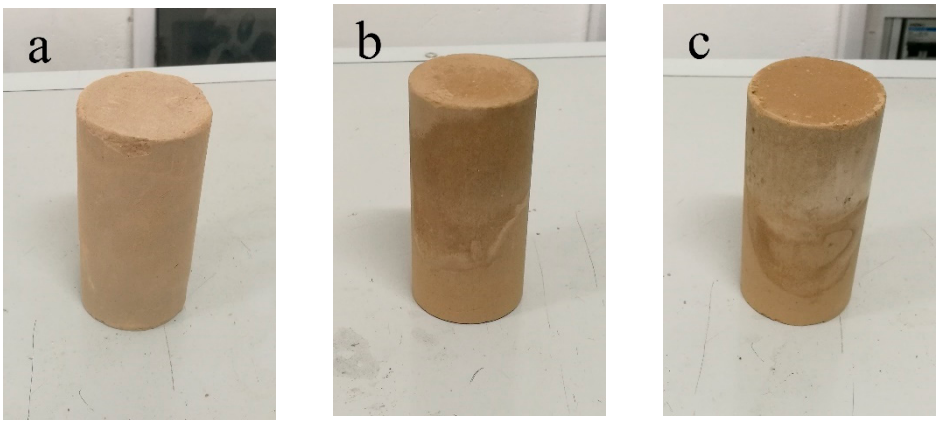

(**a**) (**b**) (**c**)

 doi:10.20944/preprints202404.0835.v1

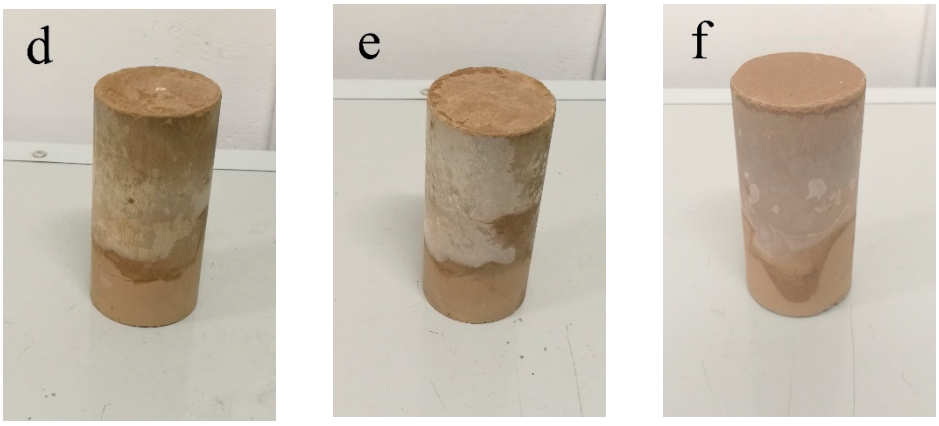

(**d**) (**e**) (**f**)

Figure 1. Remolded loess specimens treated with different concentrations of DAP. (**a**) Untreated; (**b**) 0.5 mol/L DAP; (**c**) 1.0 mol/L DAP; (**d**) 1.5 mol/L DAP; (e) 2.0 mol/L DAP; (f) 3.0mol/L DAP.

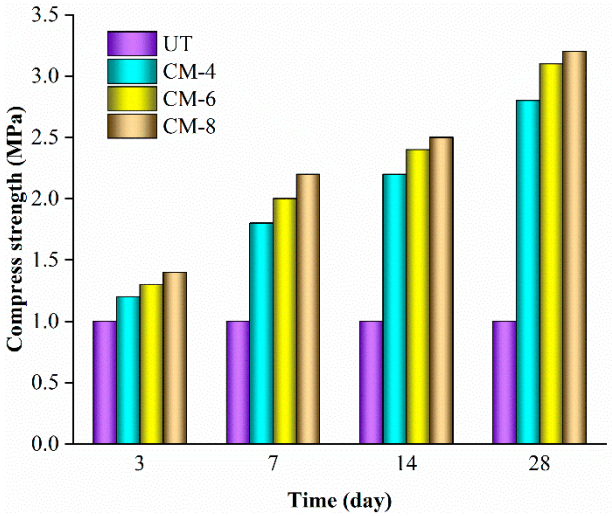

Figure 2. Compressive strength of cement-treated loess specimens.

For any specific curing age, the compressive strength of the cement-treated loess rose correspondingly with a higher dosage of cement. This is because a higher cement content results in a greater quantity of hydration products formed during the hydration process, which consequently leads to higher compressive strength. For instance, after 28 days, the compressive strengths recorded for the CM-4, CM-6, and CM-8 groups were measured to be 2.73 MPa, 2.99 MPa, and 3.08 MPa, respectively. These values represent increases of 173%, 199%, and 208% compared to the untreated group (UT), respectively.

Figure 3 depicts the compressive strength results for the DAP-treated loess specimens. According to Figure 3, aside from the control group (UT) with minimal variation, the compressive strength of the DAP-treated loess specimens progressively increased as the curing age extended. For instance, the DT-3.0 group reached a strength of 5.68 MPa at 28 days, marking a 43.07% increase from its strength at 3 days. The specimens exhibited relatively high early-stage strength, with rapid development initially, however, the rate of strength development diminished after 14 days. For example, the compressive strength of the DT-2.0 group at 28 days showed only a 14% increment compared to its compressive strength at 14 days.

 doi:10.20944/preprints202404.0835.v1

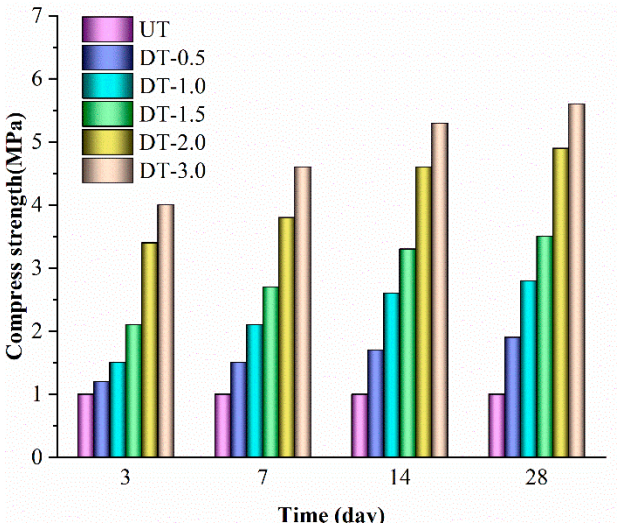

Figure 3. Compressive strength of DAP-treated loess specimens.

The concentration of DAP is a primary factor that influences the compressive strength of DAP-treated loess. Increasing the DAP concentration, that is, increasing the amount of DAP added, significantly enhanced the uniaxial compressive strength of the specimens. For loess with a high calcium content, appropriately raising the concentration of DAP can hasten the development of early-stage strength of the treated soil. For instance, at a curing age of 3 days, in comparison to the UT group, the compressive strengths measurements for the DT-0.5, DT-1.0, DT-1.5, DT-2.0, and DT-3.0 groups were 1.22 MPa, 1.49 MPa, 2.06 MPa, 3.42 MPa, and 3.97 MPa, respectively, corresponding to increases of 22%, 49%, 106%, 242%, and 297%.

In comparison to cement-treated loess, when the admixture content is comparable, DAP-treated samples exhibited significantly higher compressive strength. For example, the compressive strength at 28 days for the DT-2.0 was 14% greater than that of the CM-4, and the DT-3.0 group's compressive strength surpassed that of the CM-4 group by 29%. As the concentration of DAP rose, there was a considerable impact on the effectiveness of DAP stabilization; more HAP complexes were formed with the calcium in the soil. These complexes not only strengthened the bonding between particles but also continuously filled the pores in loess, rendering the soil sample denser. Consequently, significant enhancement was observed in the compressive strength of the loess.

The most significant increase in compressive strength occurred when the DAP solution concentration was within the range of 1.5-2.0 mol/L (corresponding to a solid content of 3-4%) after curing. Although cement also enhanced bonding during curing, its hydration process involved some shrinkage, which constrained its pore-filling capacity. As a result, this resulted in a less pronounced increase in the sample's compressive strength compared to DAP-treated loess specimens.

 doi:10.20944/preprints202404.0835.v1

3.2. Permeability and Porosity

Table 4 shows the void ratios and permeability coefficients of loess treated with different amounts of cement/DAP after 14 days. The experiments measured the time intervals (t_1-t_2) required for the water head to drop by 20cm, as well as calculation of the permeability coefficient k_T. The results indicated that both cement and DAP treatment significantly reduced the loess's permeability coefficient. After 14 days, the permeability coefficient of untreated loess was 2.42×10^{-4} cm/s; it decreased to 0.59×10^{-4} cm/s for CM-6 group; and to 0.28×10^{-4} cm/s for DT-3.0 group. Under the same admixture content conditions, the void ratio of DAP-treated loess was reduced by 0.029 compared to cement-treated loess, and there was a 52.5% decrease in the permeability coefficient, indicating that the HAP complexes generated significantly reduced the interconnected pores in the collapsible loess.

Table 4. Results of the Loess Permeability Test (14 d curing).

Groups	UT	CM-4	CM-6	CM-8	DT-1.5	DT-2.0	DT-3.0
Void ratio	0.542	0.525	0.518	0.505	0.502	0.493	0.489
Time (s)	18	40	74	105	98	126	189
Permeability coefficient (10^{-4}cm/s)	2.42	1.08	0.59	0.41	0.44	0.34	0.28

Table 5 presents the void ratios and permeability coefficients of loess treated with the same amount of cement and DAP at different curing ages. The data indicated that the void ratio of DAP-treated loess continuously diminished as curing time increased, whereas the change in void ratio for cement-treated soil was relatively small during the curing process. This is attributed to the ongoing reaction between phosphate ions from the DAP solution and the calcite present in the loess, which requires an extended period. Insufficient curing time can result in the dissolution and migration of the formed amorphous, unstable calcium phosphate and unreacted phosphate ions. Therefore, as the curing age progressed, more HAP was generated within the DAP-treated loess, leading to a reduction in both the void ratio and the permeability coefficient of the specimens. For instance, the permeability coefficient of DT-3.0 group was 0.31×10^{-4} cm/s at 3 days, and it decreased to 0.13×10^{-4} cm/s at 28 days, representing a reduction of 58%.

Table 5. Results of the Loess Permeability Test (different curing ages).

Groups	CM-6 3d	CM-6 14d	CM-6 28d	DT-3.0 3d	DT-3.0 14d	DT-3.0 28d
Void ratio	0.523	0.518	0.519	0.496	0.489	0.485
Time (s)	78	74	84	143	189	327
Permeability coefficient (10^{-4}cm/s)	0.56	0.59	0.52	0.31	0.28	0.13

3.3. Micro-Mechanism of DAP Stabilization

In addition to the considerable amount of quartz that constitutes the large particles, the loess also contains a wealth of ultra-fine carbonates, mainly existing as calcite ($CaCO_3$) and a minor amount of dolomite ($CaMg(CO_3)_2$), as shown in Table 1. The clay minerals containing Al and Fe within the loess can also react with DAP [34]. During these reactions, the bonding between the particles was enhanced and the pores were filled, which consequently increased the compressive strength of the loess.

Figure 4 illustrates the XRD pattern for the untreated loess. Apart from the peaks of quartz, analysis using standard PDF cards confirmed that the loess contained a substantial amount of calcite. This calcite can react with the added DAP solution to form HAP complexes, which served to stabilize the soil. Figure 5 depicts SEM images of the untreated remolded loess sample. Figure 6 illustrates the three predominant pore types found within the loess.

Preprints.org (www.preprints.org) | NOT PEER-REVIEWED | Posted: 12 April 2024 doi:10.20944/preprints202404.0835.v1

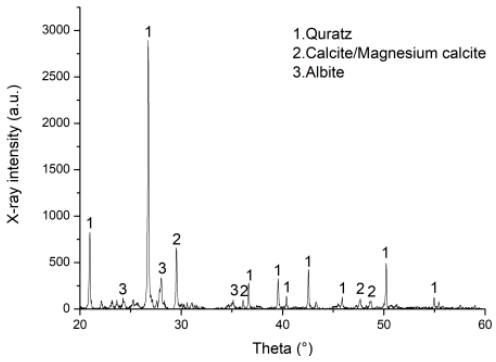

Figure 4. XRD patterns of untreated loess.

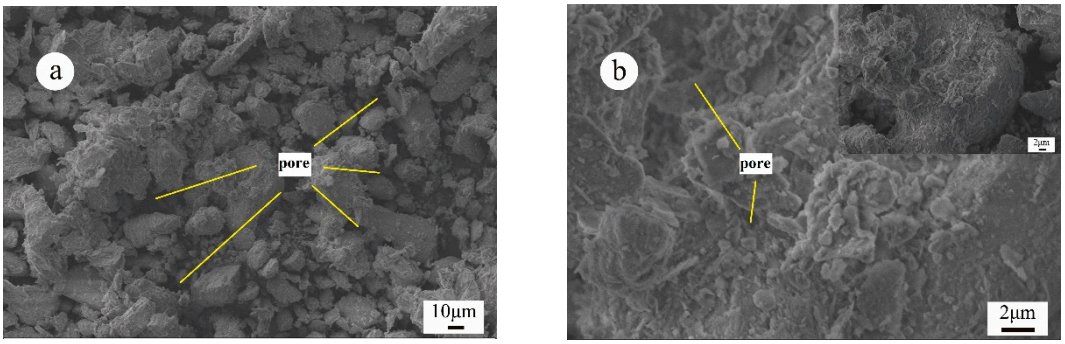

(**a**) (**b**)

Figure 5. SEM images of untreated loess. (**a**) Pore structure in loess; (**b**) Surface morphology of loess particles.

(**a**) (**b**) (**c**)

Figure 6. Pore type of loess. (**a**) Scaffold pores; (**b**) Inlaid pores; (**c**) Pores in bonding.

Figure 5 reveals that the particle surfaces are also relatively smooth. The loess particles exhibited aggregate envelopes on their surfaces, which adhered small amounts of needle-shaped or plates-shaped debris of clay minerals. In Figure 6, the scaffold pores, are large and interconnected, exhibiting pronounced instability within which various debris of clay materials partially fill (Figure 6(a)). While the inlaid pores are smaller in size and more stable, less prone to failure after soaking (Figure 6(b)). Furthermore, various micro-pores are also commonly found in bonding materials, impacting the water stability of soil (Figure 6(c)). The pores of collapsible loess are primarily composed of scaffold pores. After water immersion, seeping flow will erode and destroy these interconnected structures in soil, when subjected to its own weight or certain external pressures. The clay debris adhered to the pore walls also became dispersed and migrated into the surrounding pores, resulting in the collapse and size reduction of the large interconnected pores [6]. The inherent strength and low water stability of the loess contribute to the phenomenon of wet collapse in the loess.

 doi:10.20944/preprints202404.0835.v1

From the foregoing discussion, it can be deduced that the microstructure of untreated loess exhibits characteristics of large interconnected scaffold pores with minimal bonding, and the pores surrounding the soil particles are clearly visible. Within the loess, the interaction between particles primarily occurred through point-to-point or point-to-edge connections. The limited contact areas between particles, with only scattered bonding agents, contributed to the lower strength of the inter-particle bonding.

Figure 7 illustrates the SEM images and EDX results of loess samples treated with DAP concentrations of 1.0, 2.0, and 3.0 mol/L, following a curing period of 3 days, at a magnification of 20 μm. It was indicated that calcium ions in the loess can effectively adsorb and combine with phosphate ions from the DAP solution, leading to co-precipitation reactions that yield HAP complexes. The amount of phosphorus absorbed by calcite in the loess increased as DAP concentration rose. The samples that underwent treatment using 3.0 mol/L DAP exhibited the highest phosphorus adsorption. In the SEM images accompanying the EDX results, the relative volume of the aggregates was small. The integrity of the substantial inter-particle bonding material was compromised when the loess sample was pulverized into powder, leaving behind the relatively smaller minerals adhering to the particle surfaces. The increased strength of the loess specimens is due to the enhanced bonding between particles resulting from the reaction of DAP with calcite, which produces HAP within the loess.

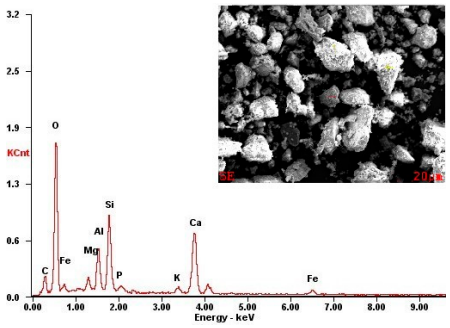

(**a**)

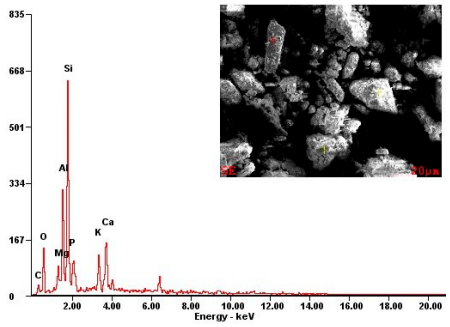

(**b**)

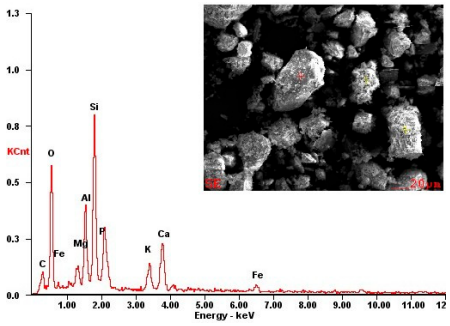

(**c**)

 doi:10.20944/preprints202404.0835.v1

Figure 7. SEM images and EDX results of loess specimens treated with different contents of DAP. (**a**)1.0mol/L, (**b**)2.0mol/L, (**c**)3.0mol/L.

The SEM observations revealing the absorption of phosphorus and its precipitation on the surface of soil particles, along with the formation of calcium phosphate precipitates, are presented in Figures 8 and 9. Specifically, Figure 8 depicts the results after 3 days of curing for different DAP concentrations. At a lower DAP concentration (0.5 mol/L), it was difficult to observe HAP complexes on the soil particle surfaces (Figure 8(a)). The comparatively lower Ca/P molar ratio, resulted in the formation of precursor and amorphous phase, distinct from HAP, with poor abilities of bonding and higher solubility [35]. Comparatively, at a higher DAP concentration (2.0 mol/L) and Ca/P molar ratio, the surface of the soil particles clearly exhibited the presence of precipitated HAP complexes with a distinct nanoscale spatial structure [26] and strong bonding strength [14] (Figure 8(d)). Figure 8 also reveals the appearance of many new small aggregates on the surface of the particles in the loess. It is because the various debris materials around the particles were bonded or even enveloped by the HAP complexes in the soil. As the concentration of DAP increased, more HAP complexes were generated, leading to an improvement on interparticle bonding and adhesiveness of the clay debris. Additionally, the debris also helped to fill the pores between the loess particles, thereby augmenting both the loess's strength and its resistance to water.

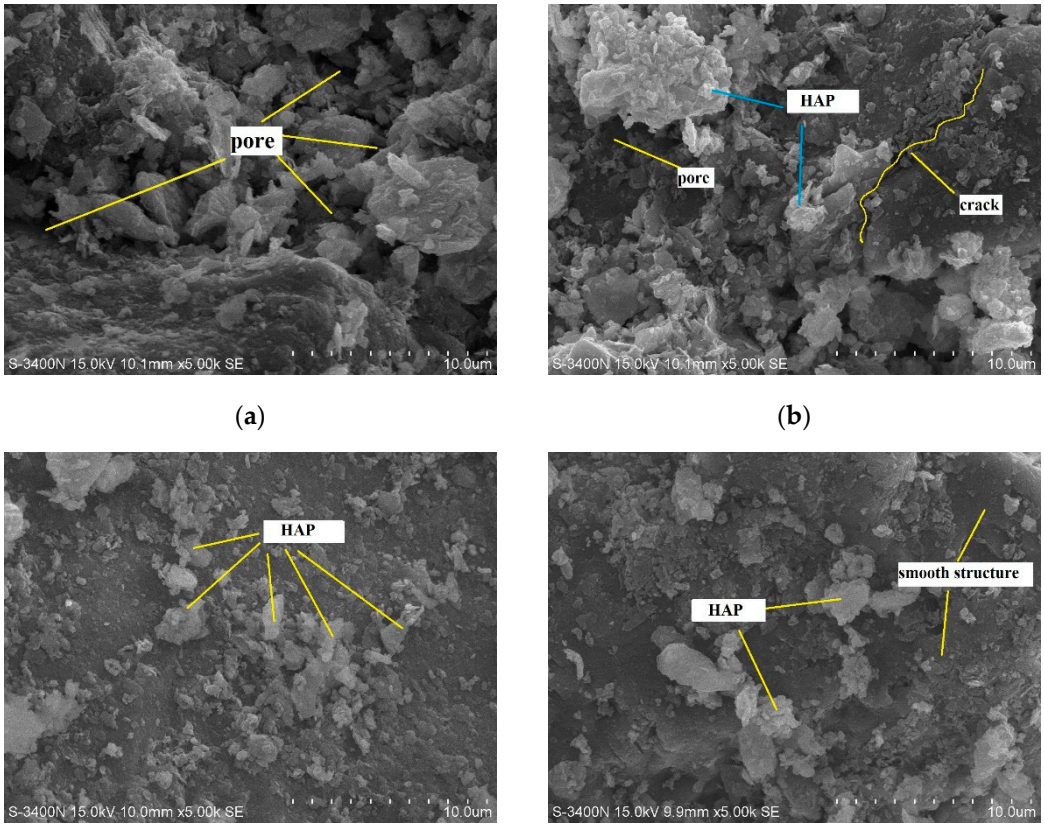

Figure 8. SEM images of loess specimens treated with different contents of DAP for 3d curing. (**a**) 0.5 mol/L; (**b**) 1.0 mol/L; (**c**) 1.5 mol/L; (**d**) 2.0 mol/L.

 doi:10.20944/preprints202404.0835.v1

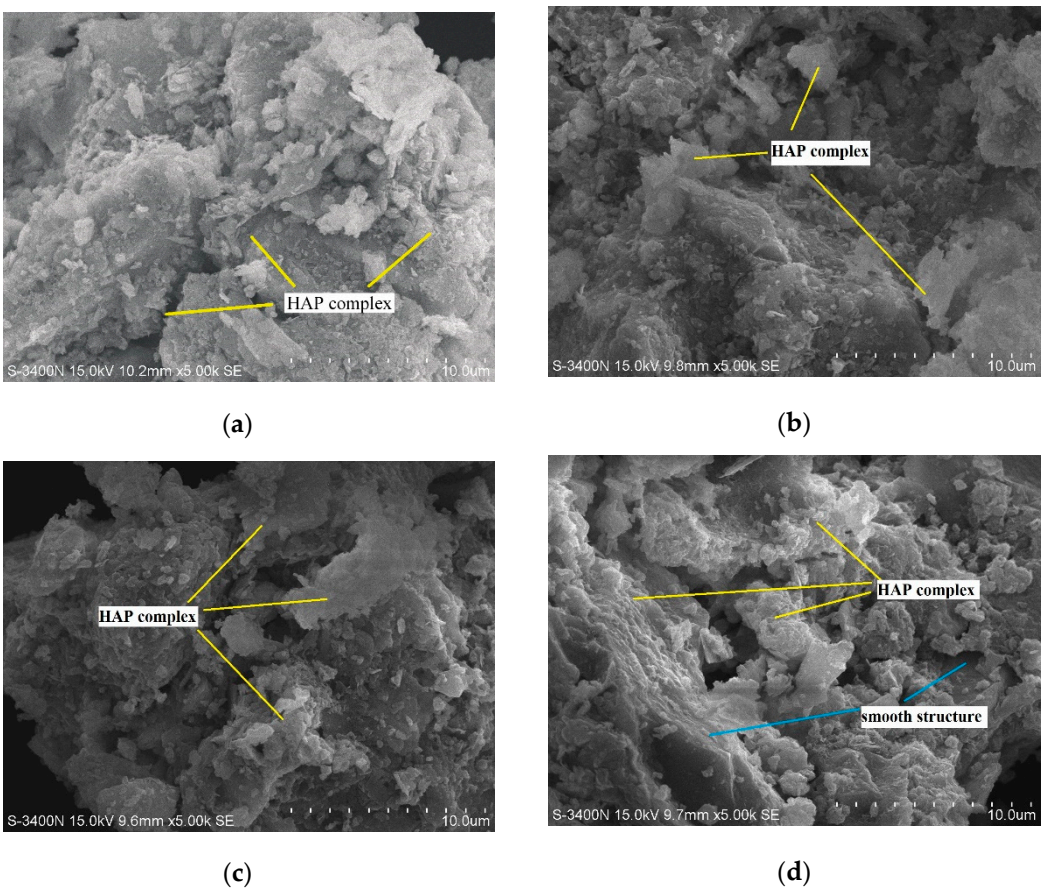

Figure 9. SEM images of DAP-treated loess specimens treated with 3.0 mol/L DAP at different curing ages (**a**) 3d; (**b**) 7d; (**c**) 14d; (**d**) 28d.

Figure 9 shows the SEM images of loess treated with 3.0 mol/L DAP at different curing ages. The longer curing age significantly promoted the accumulation of HAP complexes within the treated loess. A large amount of HAP complexes with special reticular structures precipitated between the soil particles. These precipitates bonded the soil particles together into large aggregates, thus enhancing the loess's compressive strength of the. In Figure 9(d), the pores structure has changed to inlaid contact or direct contact, as seen in Figure 6(b), in the loess treated with 3 mol/L DAP after 28-day curing. Soil particles was bonded by a large amount of HAP complexes, leading to a notable enhancement in the loess's compressive strength. Further analysis of the SEM images from groups with shorter curing ages, such as those shown in Figure 9(a) and 9(b). It was pictorial evident that the HAP complex's web-like structure around and atop the particle surfaces was more clearly in the groups with longer curing ages.

The precipitated HAP complexes not only exhibited lower solubility and better water stability than calcite [25], but also adhered more debris clay minerals in loess [34]. These complexes filled the pores between soil particles or acted as binding agents, improving the pore structure within the loess. This process enhanced the loess's compressive strength and reduced its permeability coefficient, rendering it denser and more stable. Consequently, the collapsibility of loess is significantly mitigated.

3.4. Carbon Emissions and Cost Analysis

The production and transportation of cement are associated with substantial carbon emissions, which can cause a warming effect on the environment attributed to stabilizing loess [37]. Table 6 lists the CO_2 emissions and costs associated with the use of cement and DAP for modifying and reinforcing loess. A comparative analysis revealed that the carbon emissions resulting from cement were significantly higher than those from DAP, while the material cost of DAP is relatively higher.

 doi:10.20944/preprints202404.0835.v1

For instance, to increase the 28-day compressive strength of 1 kg loess to exceed 3 MPa, CM-6 required 60g of cement, resulting in a carbon emission of 50.4g and a cost of 0.0512 RMB; in contrast, DT-1.5 required 33.7g of DAP, with a significantly lower carbon emission of 16.8g and a cost of 0.2337 RMB. While the use of DAP for reinforcing loess does indeed increase the cost, it significantly reduced the carbon emission by 33.6g per kilogram of loess stabilized, representing a 66.7% decrease in carbon emissions compared to cement modification. These findings suggest that despite the higher material cost of DAP, using it to reinforce loess offers a significant advantage in terms of reducing carbon emissions, presenting a more competitive alternative for eco-friendly and sustainable development.

Table 6. Carbon emissions of cement and DAP production and their market price.

Raw Materials	Carbon Emission Factor (kg CO_2/kg)	Market Price (RMB/kg)
OPC	0.84	0.64
DAP	0.50	3.80

4. Conclusions

As an innovative, eco-friendly soil modification agent, DAP release phosphate ions that react with the carbonates in the collapsible loess, generating HAP complex precipitates around the soil particles, enhancing its strength and water stability. Compared to traditional cement, the use of DAP for soil stabilization yields a more notable improvement in strength, a greater reduction in the coefficient of permeability, and a more significant decrease in carbon emissions. From the outcomes and analysis, the following conclusions can be formulated:

1. Unconfined compressive tests suggest that DAP has a better stabilization effect on loess than Portland cement. Loess treated with a 3.0 mol/L DAP solution showed a significant in maximum compressive strength by 297% after a 28-day curing period. Holding the solid content constant, DAP-treated loess exhibited a 14-29% greater compressive strength than that of cement-treated loess.
2. HAP complexes are also more effective than cement in reducing interconnected pores within loess. The permeability coefficient of DT-3.0 was 0.31×10^{-4} cm/s at 3 days, and decreased to 0.13×10^{-4} cm/s at 28 days. As the curing age increases, there is a notable decrease of 58% in permeability coefficient of DAP-treated loess. Under the same solid content, the permeability coefficient of DAP-treated loess is 52.5% lower than that of cement-treated loess.
3. SEM/EDX analysis showed that DAP reacted with the calcium carbonate in loess, leading to the formation of HAP during curing. This reaction improved the interparticle bonding and filled the pores within loess, strengthening its structure and significantly increasing its compressive strength. The curing time is pivotal for effectively promoting the development and bonding strength of HAP complexes within the treated loess. After 28 days, a large amount of distinct nanoscale reticular structures of HAP complexes can be observed between the soil particles, enveloping both the particles and clay debris.
4. As an innovative agent for soil stabilization, DAP holds the promise to replace traditional cement and lime in the stabilization of collapsible loess. According to carbon emission and cost analysis, DAP offers superior environmental advantages over cement, with a significant reduction in carbon emissions by 68%. Considering the solubility of DAP in water, it is recommended to employ 3.0 mol/L DAP solution for the effective stabilization of loess.

Author Contributions: Conceptualization, L.H. and H.C.; methodology, L.H.; validation, C.Y., L.H. and Y.Z.; formal analysis, C.Y. and L.H.; investigation, C.Y. and L.H.; resources, H.C. and D.Y.; data curation, L.H. and Y.Z.; writing—original draft preparation, C.Y. L.H. and Y.Z.; writing—review and editing, C.Y. and H.C.; visualization, L.H. and Y.Z.; supervision, D.Y.; project administration, H.C. All authors have read and agreed to the published version of the manuscript.

Funding: This research was funded by the National Natural Science Foundation of China (Project Nos 41440018 and 41672278).

 doi:10.20944/preprints202404.0835.v1

Data Availability Statement: The data presented in this study are available on request from the corresponding author due to confidentiality reasons.

Acknowledgments: The authors gratefully acknowledge the support from the National Natural Science Foundation of China (Project Nos 41440018 and 41672278).

Conflicts of Interest: The authors declare that the research was conducted in the absence of any commercial or financial relationships that could be construed as a potential conflict of interest.

References

1 Liu, D. S. Loess and environment. *Journal of Xi'an Jiaotong University(Social Sciences Edition)* **2002**.
2 Li, P. Y.; Qian, H.; Wu, J. H. Environment: accelerate research on land creation. *Nature* **2014,** *510* (7503), 29.
3 Liu, X. J.; Pan, C. F.; Yu, J.; Fan, J. Y. Study on micro-characteristics of microbe-induced calcium carbonate solidified loess. *Crystals* **2021,** *11* (12), 12.
4 Li, Z. X.; Wang, J. D.; Yang, S.; Liu, S. H.; Li, Y. W. Characteristics of microstructural changes of malan loess in yan'an area during creep test. *Water* **2022,** *14* (3), 22.
5 Zheng, Z. Y.; Li, X. A.; Wang, L.; Li, L. C.; Shi, J. F.; Bi, M. L. A new approach to evaluation of loess collapsibility based on quantitative analyses of colloid-clay coating with statistical methods. *Engineering Geology* **2021,** *288*, 12.
6 Liu, Z.; Liu, F. Y.; Ma, F. L.; Wang, M.; Bai, X. H.; Zheng, Y. L.; Yin, H.; Zhang, G. P. Collapsibility, composition, and microstructure of loess in China. *Canadian Geotechnical Journal* **2015,** *53* (4), 673.
7 Gao, C. H.; Du, G. Y.; Liu, S. Y.; He, H.; Zhang, D. W. The microscopic mechanisms of treating collapsible loess with vibratory probe compaction method. *Transportation Geotechnics* **2021,** *27*.
8 Ge, M. M.; Pineda, J. A.; Sheng, D. C.; Burton, G. J.; Li, N. Microstructural effects on the wetting-induced collapse in compacted loess. *Computers and Geotechnics* **2021,** *138*, 14.
9 Ikeagwuani, C. C.; Obeta, I. N.; Agunwamba, J. C. Stabilization of black cotton soil subgrade using sawdust ash and lime. *Soils and Foundations* **2019,** *59* (1), 162.
10 Mahedi, M.; Cetin, B.; White, D. J. Cement, lime, and fly ashes in stabilizing expansive soils: performance evaluation and comparison. *Journal of Materials in Civil Engineering* **2020,** *32* (7), 16.
11 Horpibulsuk, S.; Rachan, R.; Suddeepong, A. Assessment of strength development in blended cement admixed Bangkok clay. *Construction and Building Materials* **2011,** *25* (4), 1521.
12 Lemaire, K.; Deneele, D.; Bonnet, S.; Legret, M. Effects of lime and cement treatment on the physicochemical, microstructural and mechanical characteristics of a plastic silt. *Engineering Geology* **2013,** *166*, 255.
13 Hou, Y. F.; Li, P.; Xiao, T.; H., H. R. *Review on strengthening loess with curing agents*; Journal of Engineering Geology, 2019.
14 Possenti, E.; Colombo, C.; Conti, C.; Gigli, L.; Merlini, M.; Plaisier, J. R.; Realini, M.; Sali, D.; Gatta, G. D. Diammonium hydrogenphosphate for the consolidation of building materials. Investigation of newly-formed calcium phosphates. *Construction and Building Materials* **2019,** *195*, 557.
15 Wang, Y.; Guo, C. H.; Chen, X. J.; Jia, L. Q.; Guo, X., N.; Chen, R. S.; Zhang, M. S.; Chen, Z. Y.; Wang, H. D. Carbon peak and carbon neutrality in China: Goals, implementation path and prospects. *China Geology* **2021,** *4* (4), 720.
16 Zhang, F. Y.; Pei, X. J.; Yan, X. D. Physicochemical and mechanical properties of lime-treated loess. *Geotechnical and Geological Engineering* **2017,** *36* (1), 685.
17 Ravindran, G.; Bahrami, A.; Mahesh, V.; Katman, H. Y. B.; Srihitha, K.; Sushmashree, A.; Kumar, A. N.; Far, H. Global research trends in engineered soil development through stabilisation: scientific production and thematic breakthrough analysis. *Buildings* **2023,** *13* (10), 17.
18 Ikeagwuani, C. C.; Nwonu, D. C. Emerging trends in expansive soil stabilisation: A review. *Journal of Rock Mechanics and Geotechnical Engineering* **2019,** *11* (2), 423.
19 Yang, F. W.; Zhang, B. J.; Liu, Y.; Wei, G. F.; Zhang, H.; Chen, W. X.; Xu, Z. Biomimic conservation of weathered calcareous stones by apatite. *New Journal of Chemistry* **2011,** *35* (4), 887.
20 Song, J.; Ma, J. X.; Li, F. Y.; Chai, L. N.; Chen, W. F.; Dong, S.; Li, X. J. Study on fractal characteristics of mineral particles in undisturbed loess and lime-treated loess. *Materials* **2021,** *14* (21).
21 Li, X. A.; Sun, J. Q.; Ren, H. Y.; Lu, T.; Ren, Y. B.; Pang, T. The effect of particle size distribution and shape on the microscopic behaviour of loess via the DEM. *Environmental Earth Sciences* **2022,** *81* (10), 290.
22 Nan, Y. L.; Wei, Y. N.; Liu, K.; Cao, Y. B. Quantitative 3D characterization of pore structure in malan loess from different regions of the loess plateau. *Water* **2023,** *15* (17), 14.
23 Jiang, M. J.; Zhang, F. G.; Hu, H. J.; Cui, Y. J.; Peng, J. B. Structural characterization of natural loess and remolded loess under triaxial tests. *Engineering Geology* **2014,** *181*, 249.
24 Matteini, M.; Rescic, S.; Fratini, F.; Botticelli, G. Ammonium phosphates as consolidating agents for carbonatic stone materials used in architecture and cultural heritage: preliminary research. *International Journal of Architectural Heritage* **2011,** *5* (6), 717.

 doi:10.20944/preprints202404.0835.v1

25 Sassoni, E.; Naidu, S.; Scherer, G. W. The use of hydroxyapatite as a new inorganic consolidant for damaged carbonate stones. *Journal of Cultural Heritage* **2011,** *12* (4), 346.

26 Sassoni, E.; D'Amen, E.; Roveri, N.; Scherer, G. W.; Franzoni, E. Durable self-cleaning coatings for architectural surfaces by incorporation of Tio2 nano-particles into hydroxyapatite films. *Materials* **2018,** *11* (2), 16.

27 Eliassi, M. D.; Zhao, W.; Tan, W. F. Effect of carbonate and phosphate ratios on the transformation of calcium orthophosphates. *Materials Research Bulletin* **2014,** *55*, 114.

28 Uskokovic, V.; Odsinada, R.; Djordjevic, S.; Habelitz, S. Dynamic light scattering and zeta potential of colloidal mixtures of amelogenin and hydroxyapatite in calcium and phosphate rich ionic milieus. *Archives of Oral Biology* **2011,** *56* (6), 521.

29 Ion, R.-M.; Turcanu-Caruțiu, D.; Fierăscu, R.-C.; Fierăscu, I.; Bunghez, I.-R.; Ion, M.-L.; Teodorescu, S.; Vasilievici, G.; Rădiţoiu, V. Caoxite-hydroxyapatite composition as consolidating material for the chalk stone from Basarabi–Murfatlar churches ensemble. *Applied Surface Science* **2015,** *358*, 612.

30 Yang, F. W.; Liu, Y. Artificial hydroxyapatite film for the conservation of outdoor marble artworks. *Materials Letters* **2014,** *124*, 201.

31 Sena da Fonseca, B.; Ferreira Pinto, A. P.; Piçarra, S.; Caldeira, B.; Montemor, M. F. Consolidating efficacy of diammonium hydrogen phosphate on artificially aged and naturally weathered coarse-grained marble. *Journal of Cultural Heritage* **2021,** *51*, 145.

32 Sassoni, E.; Graziani, G.; Franzoni, E. An innovative phosphate-based consolidant for limestone. Part 1: Effectiveness and compatibility in comparison With ethyl silicate. *Construction and Building Materials* **2016,** *102*, 918.

33 Wang, L.; Nancollas, G. H. Calcium Orthophosphates: Crystallization and Dissolution. *Chemical Reviews* **2008,** *108* (11), 4628.

34 Li, W.; Xu, W. Q.; Parise, J. B.; Phillips, B. L. Formation of hydroxylapatite from co-sorption of phosphate and calcium by boehmite. *Geochimica Et Cosmochimica Acta* **2012,** *85*, 289.

35 Wang, L. J.; Nancollas, G. H. Calcium orthophosphates: crystallization and dissolution. *Chemical Reviews* **2009,** *108* (11), 4628.

36 GB/T 50123-2019. Ministry of Housing and Urban Rural Development of the People's Republic of China. *Geotechnical test methods standard*. State Administration for Market Regulation, **2019**. Beijing, China.

37 Nie, S.; Zhou, J.; Yang, F.; Lan, M.; Li, J.; Zhang, Z.; Chen, Z.; Xu, M.; Li, H.; Sanjayan, J. G. Analysis of theoretical carbon dioxide emissions from cement production: Methodology and application. *Journal of Cleaner Production* **2022,** *334*, 130270.